Competency of Certain Natural Products as Inhibitors for SARS-CoV-2: the In-silico Exploration

Seema Shukla[1], Anubha Srivastava[2,*], Poonam Tandon[2,*], and Rajendra Bahadur Singh[2]

[1]*Government Degree College Mant, Mathura, 281202, Uttar Pradesh, India*

[2]*Department of Physics, University of Lucknow, Lucknow, 226 007, Uttar Pradesh, India.*

Abstract: *Abundance of natural products in edible plants and their vast role in the treatment of almost all the diseases is the motivation behind the investigation of their candidature as inhibitor for COVID-19. Seven selected natural products named, (1) bicuculline, (2) boldine, (3) 1-(4-chlorophenyl)-3-(5-methylfuran-2-yl) prop-2-en-1-one, (4) piplartine, (5) formononetin, (6) isoformononetin, and (7) tectorigenin, were first examined for drug likeness and reactivity. The activity at various atomic sites has been inspected graphically through molecular electrostatic potential surface (MESP) plot and quantitative description of the same was given within the framework of conceptual DFT. The analyses of Fukui and Parr functions have exposed the similar active sites as depicted by MESP surface analysis. Furthermore, the molecular docking studies of the abovementioned compounds (inhibitor) with the main protease present in SARS-CoV-2 (6LU7) have been performed. The comparison of docking parameters such as binding affinity, inhibition constant with strength and bond-lengths of hydrogen bond had revealed that isoformononetin is the most apposite prospect for the same.*

Keywords: molecular docking; natural products; COVID-19; reactivity descriptor; molecular electrostatic potential

1. Introduction

A novel disease named COVID-19 caused by severe acute respiratory syndrome coronavirus 2 (SARS-CoV-2) [1] had been recognized in Dec 2019 in Wuhan city of China and declared as pandemic by WHO on 11 March, 2020 [2]. Since then five variants (alpha, beta, gamma, delta and omicron) of the virus have been reported and researchers are struggling to hit upon the strain of novel corona virus SARS-CoV-2 and attempting to trace a suitable inhibitor for the same. There are various COVID-19 vaccines administered and efforts are being made to trace a most effective and appropriate drug for the same. Natural products have already proven their candidacy as a drug for almost all the diseases; hence, they are emerging as potential inhibitor for many newer ailments. Due to their ease of accessibility, profusion in nature and negligible side effects they are gaining attention of researchers [3-7]. Seven such compounds named, (1) bicuculline, (2) boldine, (3) 1-(4-chlorophenyl)-3-(5-methyl furan-2-yl) prop-2-en-1-one, (4) piplartine, (5) formononetin, (6) isoformononetin, and (7) tectorigenin, have been chosen and studied for their bioactivity against SARS-CoV-2 as given in Figure 1. The vibrational spectroscopic and density functional theory (DFT) studies on these compounds have already been reported [8-14]. These reported structures were optimized using B3LYP/6-311++G(d,p) and considered for auxiliary investigations. All the seven molecules have passed the drug likeness test inspected through Lipinski's 5 rule (LR5)[15]. The frontier molecular orbital (FMO) analyses have predicted the re-activity of the seven molecules in terms of global reactivity descriptors. The graphical and topological descriptions of activity at various atomic sites of the molecules have been scrutinized via molecular electrostatic potential (MESP) surface and local reactivity descriptor analyses, respectively. Further, the blind docking of all the molecules with the main protease present in SARS-CoV-2 has been performed [16]. The docking parameters have been compared to predict the best possible inhibitor for the same.

*Corresponding author. Tel.: +91 522 2782653: Fax: +91 522 2740840;

E-mail address: poonam_tandon@yahoo.co.uk, anubhaphysics@gmail.com

2. Computational details

The geometry optimization of the initial structure was performed via DFT approach [17] implemented in Gaussian 09 [18] using B3LYP hybrid exchange correlation functional with 6-311++G(d,p) basis set [19-21]. The structure was envisaged via GaussView program [22]. The molecular mass (M), lipophilicity (Log_{10} P), number of H bond donors and acceptors, and molar refractivity (MR) have been calculated to examine LR5 [15]. In-silico molecular docking analyses have been carried out using Auto Dock 4.2 [23]. The graphical user interface of autodock tool (ADT) was used to add polar hydrogen. Atomic and partial charges were calculated using Kolloman method [24] and Geistenger method [25], respectively. The most convincing and consis- tent Lamarckian Genetic Algorithm (LGA) was implemented to discover best docked conformer which was then envisioned in the Discovery Studio Visualizer [26].

3. Results and discussions

3.1 Geometry optimization

The compounds (1) bicuculline, (2) boldine, (3) 1-(4-chlorophenyl)-3-(5-methyl furan-2-yl) prop-2-en-1-one, (4) piplartine, (5) formononetin, (6) isoformononetin, and (7) tectorigenin, have been investigated for their bioactivity against SARS-CoV-2. The DFT analyses on these structures have already validated their existence [8-14]. How- ever, they have been further optimized using B3LYP/6-311++G (d, p) level of theory. The optimized structures and atom number scheme of the compounds are presented in Figure 1. Compounds 1, 2 and 4 are isoquinoline, aporphine, and amide alkaloid, respectively; 3 is a hetero-cyclic chalcones derivative and 5-7 are iso-flavonoids [8-14]. The analysis concerning stability and binding of a ligand with a receptor are guided primarily by the 3D structure of the molecule. The aforesaid optimized structures have been used for the comparative non-empirical study concerning the bioactivity of the molecules.

3.2 Drug likeness

The first and foremost stride in the drug discovery is to check the drug likeness of the molecule that can be performed in a simplified manner through LR5 [15]. Although absorption property of a molecule and bioavailability are not directly related to each other yet the knowledge about absorption is useful parameter for bioavailability modeling. LR5 sets the criteria on M; number of H bond donor and acceptor; $\log_{10}$ P; and MR. It is a qualitative standard and does not measure oral absorption topologically. The partition function (P) illustrates the tendency of a neutral compound to dissolve in an immiscible biphasic system of lipid and water [27]. Its positive value indicates the lipophilic nature of the compound and is generally measured octan1-ol against water. MR is calculated by Lorenz-Lorentz formula given as…

$$MR = \frac{n^2-1}{n^2+1}\frac{M}{d} \quad (1)$$

Where n is the refractive index and d is density of the compound. MR is related to London dispersive force that acts in drug-receptor interaction [28, 29]. According to LR5, for drug likeness of the molecule, (i) M < 500; (ii) number of H bond donor/ acceptor < 5/10 (iii) Log_{10} P < 5 (iv) 40 ≤ MR ≤ 130 [15]. The parameters defining drug likeness are specified in Table 1. It is clear that all the seven natural products satisfy LR5, hence, are fitting in the category of drug molecule.

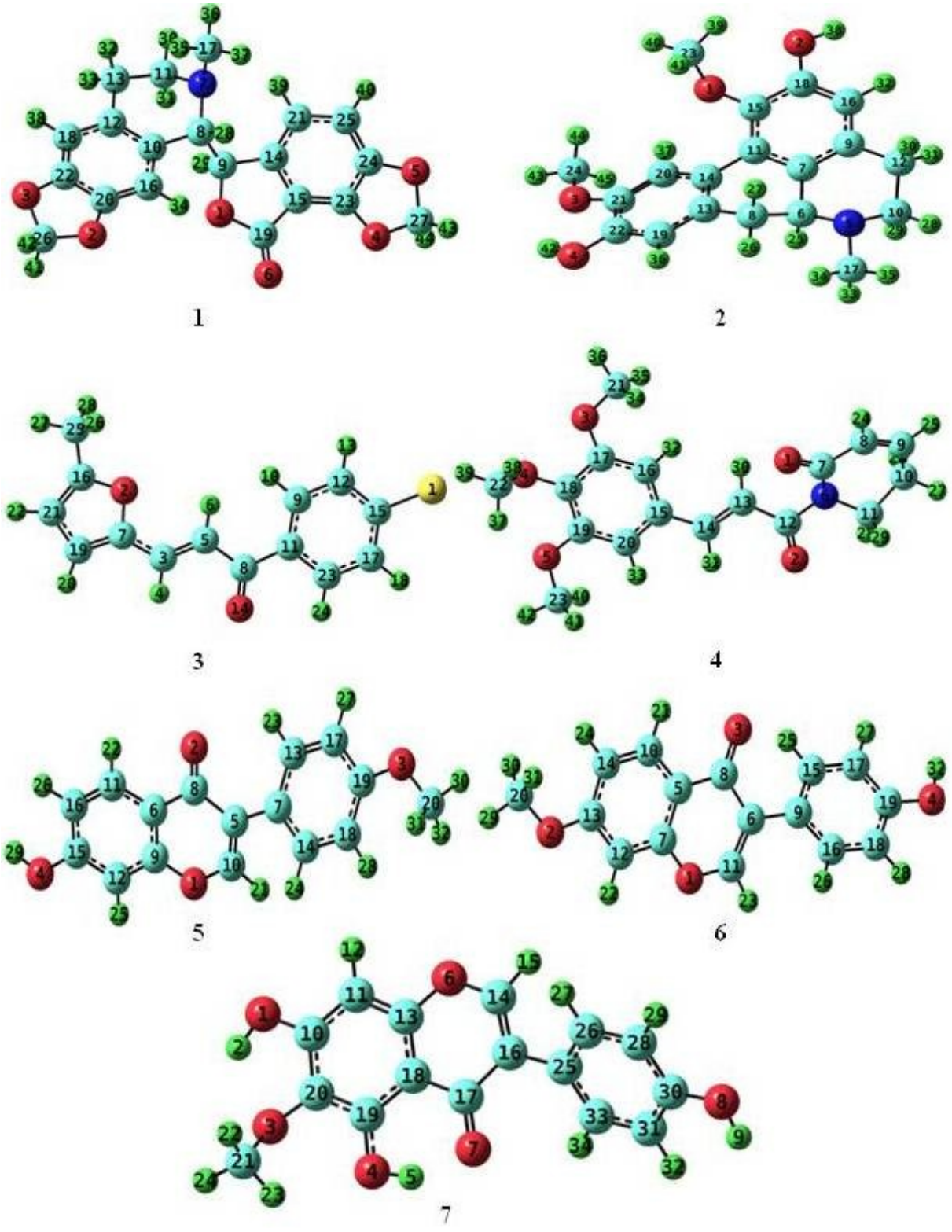

Figure 1 Optimized structure of compounds (1-7).

Table 1
Molecular mass (M); Number of H bond donor and acceptor; Log of Partition Coefficient ($\log_{10}$ P); Molar refractivity (MR) of compounds (1-7).

Compound	M	No. of H bond donor	No. of H bond acceptor	Log_{10} P	MR
1	367	0	7	0.8948	88.1330
2	327	2	5	2.8671	91.0906
3	246	0	2	4.1375	68.2615
4	317	0	6	2.0407	85.6090
5	268	1	4	3.0170	74.0363
6	268	1	4	3.0170	74.0363
7	300	3	6	2.4282	77.3659

3.3 FMO analysis and global reactivity descriptors

The reactivity of molecules can be estimated with the help of frontier molecular (FMO) orbital analysis. The global reactivity descriptors (GRD) defined in terms of energies of highest occupied molecular orbital (E_{HOMO}) and lowest unoccupied molecular orbital (E_{LUMO}) provides a quantitative assessment of reactivity of a compound [30-35]. The ionization potential (I), electron affinity (A), electronic chemical potential (μ),hardness (η), softness (S), electronegativity (χ), and the electrophilicity index (ω) ofa molecule are defined as follows...

$$I = -E_{HOMO} \quad (2)$$

$$A = -E_{LUMO} \quad (3)$$

$$\mu = -\frac{I+A}{2} \quad (4)$$

$$\eta = \frac{I-A}{2} \quad (5)$$

$$S = \frac{1}{\eta} \quad (6)$$

$$\chi = -\mu \quad (7)$$

$$\omega = \frac{\mu^2}{2\eta} \quad (8)$$

The molecular orbitals associated with HOMO and LUMO are shown in Figure 2 and the GRD are summarized in Table 2. As a first examination it is obvious from Table2 that compound 3 is most reactive with least value of E_g and highest value of S. However, the values of I, A, and χ ($-\mu$) are maximum for the aforesaid molecule, which declares that the removal or addition of an electron is hard for it. It is also inferred from Table 2 that compound 2 is most stable having largest E_g and least S. The bioactivity of these compounds can be further explored with the help of MESP plot and local reactivity descriptors as described in sections 3.4 and 3.5, respectively.

Table 2
Global reactivity descriptors of the compounds (1-7).

Comp.	E_{HOMO}	E_{LUM0}	E_g	I	A	μ	η	S	χ	ω
1	-5.8472	-1.6147	4.2325	5.8472	1.6147	-3.7310	2.1162	0.4725	3.7310	3.2889
2	-5.4733	-0.9834	4.4899	5.4733	0.9834	-3.2284	2.2449	0.4454	3.2284	2.3213
3	-6.1949	-2.5481	3.6469	6.1949	2.5481	-4.3715	1.8234	0.5484	4.3715	5.2401
4	-5.9226	-2.2199	3.7027	5.9226	2.2199	-4.0712	1.8513	0.5402	4.0712	4.4765
5	-5.9764	-1.8090	4.1674	5.9764	1.8090	-3.8927	2.0837	0.4799	3.8927	3.6361
6	-6.0151	-1.8044	4.2107	6.0151	1.8044	-3.9097	2.1053	0.4750	3.9097	3.6303
7	-6.0921	-1.9394	4.1527	6.0921	1.9394	-4.0157	2.0764	0.4816	4.0157	3.8832

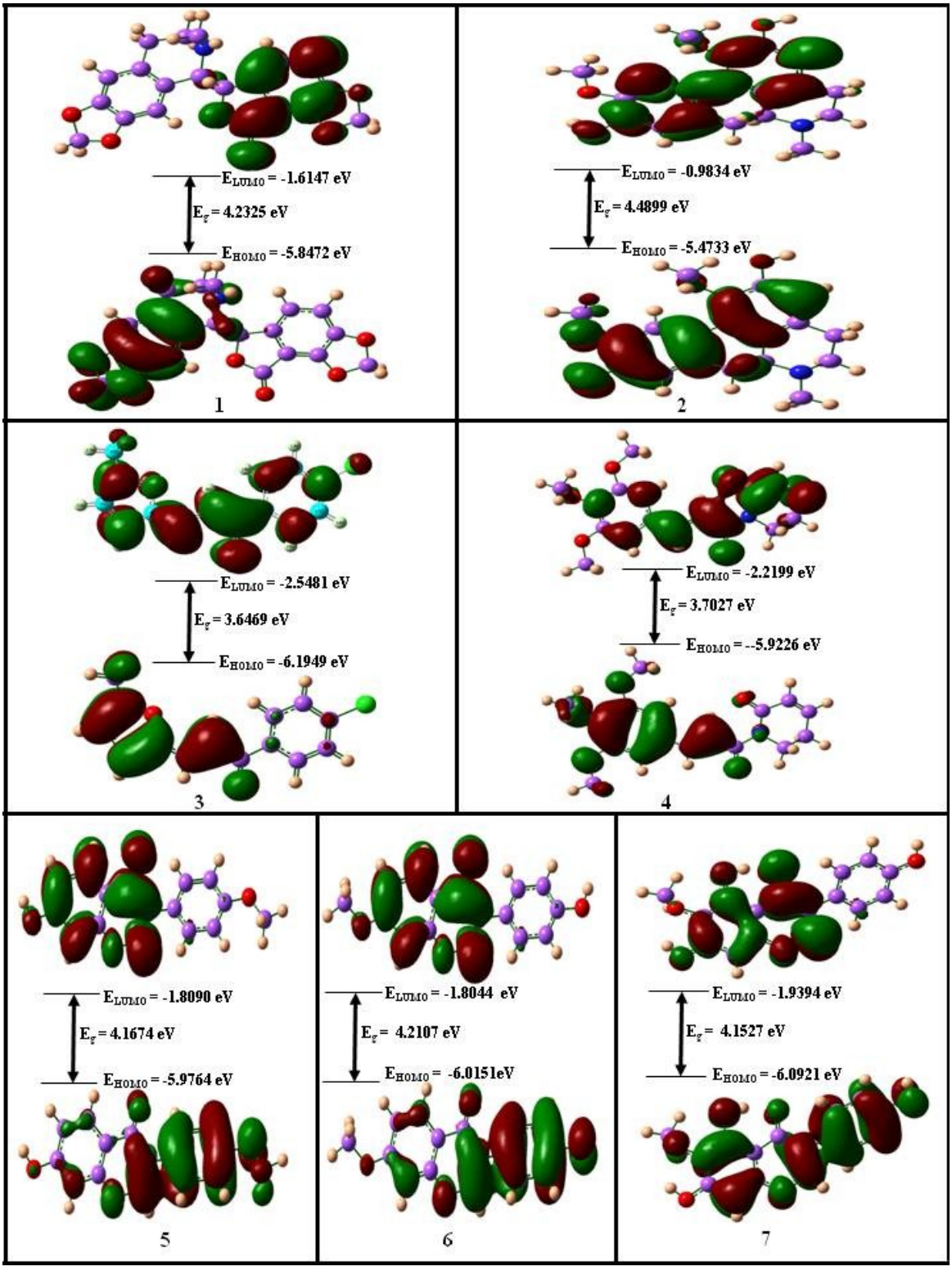

Figure 2 HOMO and LUMO orbitals of compounds (1-7).

3.4 Molecular electrostatic potential surface

The molecular electrostatic potential deals with the analysis of intermolecular interaction via transfer of charge, leading to binding of a molecule with target. The electronic component of MESP *U(r)* at a position vector r is given by Murray et al. [36] as...

$$U(r) = \int \frac{\rho(r')}{|r-r'|} dr' \quad (9)$$

Where $\rho(r')$ is the charge density at a r' The graphical representation of the activity can be very well illustrated by plotting MESP onto the total $\rho(r)$. The graph represents the region of electrophilicity and nucleophilicity in color coded form [36]. The two extremes regions i.e. red and blue are the most prominent site for electrophilic and nucleophilic attack, respectively. The MESP surface plots of the abovementioned molecules are presented in Figure 3. It could be undoubtedly envisaged from Figure 3 that (i) a red blob was visible around electronegative oxygen of the molecule such as O6, O14, (O1 & O2), O2, O3 and O7 in compounds 1, 3, 4, 5, 6 and 7, respectively; how- ever, the ring oxygen went without nucleophilicity due to charge conjugation within the aromatic ring. (ii) The hydroxyl groups present in the iso-flavonoids (5-7) were sites of nucleophilic attack (blue region) provided they were not surrounded by electron donating moiety at ortho and/or meta positions. For example, a blue region was noticeable around O4H, O4H and O8H in compounds 5, 6 and 7, respectively; however O1H in compound 7 lacks electrophilicity. (iii) Methoxy/hydroxyl group were prominent center of electrophilic attack (red region) only if additional methoxy and/or hydroxyl groups were attached in their close vicinity. It was noticed that in compound 4, O4CH3, which had methoxy groups (O3CH3 and O5CH3) at the two ortho positions, was a center of electrophilic attack. These prominent sites of electrophilicity and nucleophilicity are responsible for the hydrogen bond formation in target ligand interactions as discussed in detail under section 3.6.

3.5 Local reactivity descriptors

A topological analysis to describe the activity at various atomic sites of the molecule is described by analyzing the change in electron density and atomic spin density (ASD) with change in number of electrons at fixed potential [37]. The former are termed as Fukui functions (FF) and the latter are called Parr functions (PF). The three FF namely f_k^+, f_k^- and f_k^0 defining electrophilic, nucleophilic, and radical reactivity, respectively, for the kth atom of a molecule, can be calculated using finite difference approach [38] as...

$$f_k^+ = \rho(N_0+1) - \rho(N_0) = q_k(N_0+1) - q_k(N_0) \quad (10)$$

$$f_k^- = \rho(N_0) - \rho(N_0-1) = q_k(N_0) - q_k(N_0-1) \quad (11)$$

$$f_k^0 = \frac{\rho(N_0+1)+\rho(N_0-1)}{2} = \frac{q_k(N_0+1)+q_k(N_0-1)}{2} \quad (12)$$

Where N_0 is the number of the electrons in the ground state, and q_k is the gross charge on the kth atom of the molecule. The other local reactivity descriptors such as local softness (S_k^+, S_k^-, S_k^0); electrophilicity indices (ω_k^+, ω_k^-, ω_k^0); and relative softness (S_k^+/S_k^-, Sk^-/S_k^+) may also be derived from FF [39, 40].

$$S_k^\pm = Sf_k^\pm, \quad S_k^0 = Sf_k^0 \quad (13)$$

$$\omega_k^\pm = \omega f_k^\pm, \quad \omega_k^0 = \omega f_k^0 \quad (14)$$

The Parr functions (P_k^+ and P_k^-) proposed by Domingo et al. [41, 42] have been specified as...

$$P_k^\pm = \sigma_{sk}(N_0 \pm 1) \quad (15)$$

Where σ_{sk} is the ASD of the kth atom of the molecule; +, and - sign show nucleophilic, and electrophilic attack, respectively. The Fukui/Parr functions have been calculated by considering hirshfeld charges. The local reactivity descriptors for selected atoms of compounds (1-7) are given in Table 3. A close examination of Table 3 inferred that the values of f_k^+ / f_k^- were highest for C26/C25, O4/C24, C5/C3, C22/C14, C20/C10, O4/C11 and O8/C14, for compounds 1-7, respectively. The Fukui and Parr functions are in close resemblance and depict almost the similar sites of nucleophilicity and electrophilicity in all the molecules. The $S_k^\pm$, $\omega_k^\pm$, S_k^+/S_k^-, and S_k^-/S_k^+, providing the tendency of electrophilicity or nucleophilicity are also summarized in the Table 3.

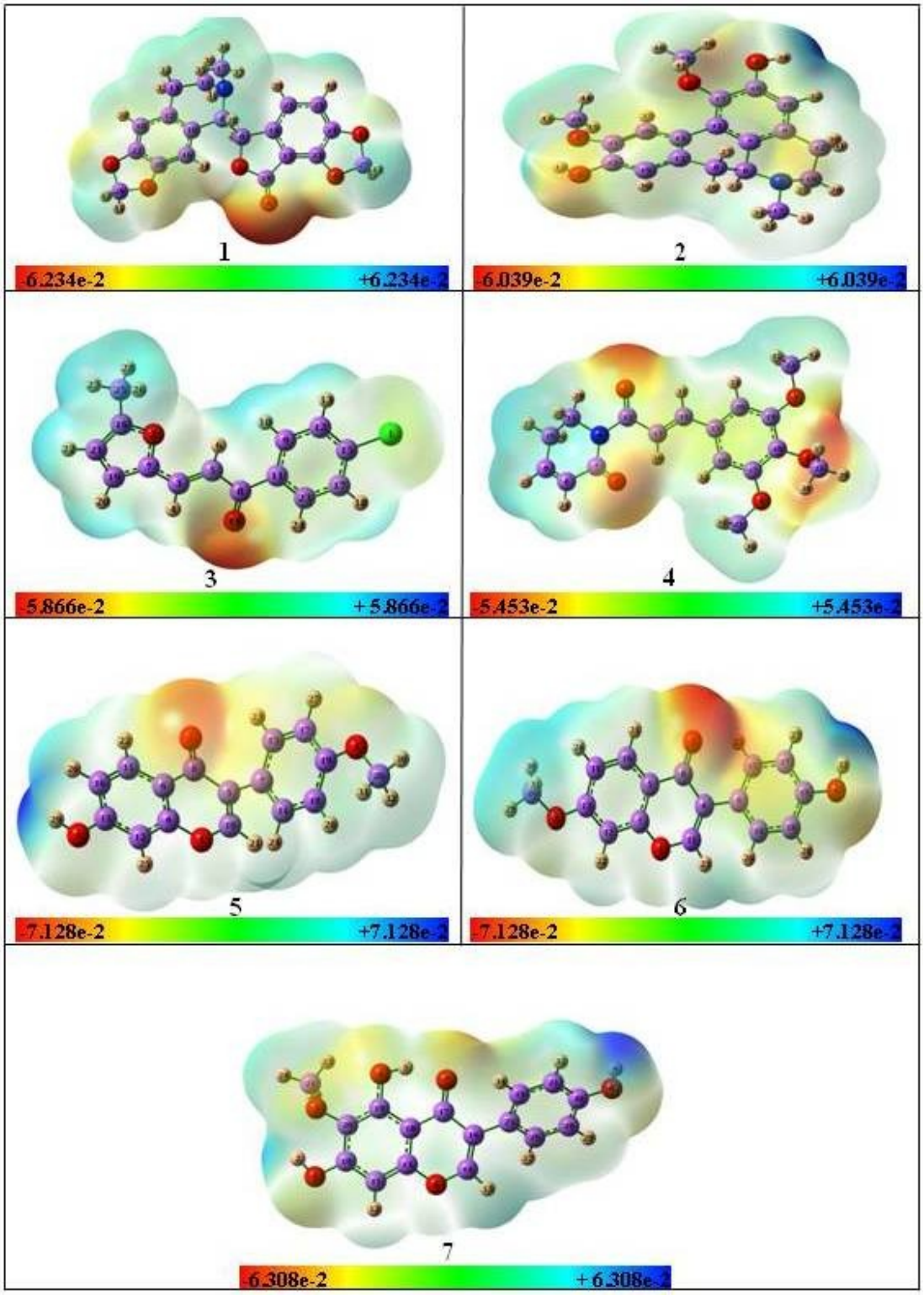

Figure 3 Molecular electrostatic potential surface plots of compounds (1-7).

Table 3
Selected local reactivity descriptors of compounds (1-7).

Comp.	Atom	f_k^+	f_k^-	f_k^0	S_k^+	S_k^-	S_k^+/S_k^-	S_k^-/S_k^+	S_k^0	ω_k^+	ω_k^-	ω_k^0	P_k^+	P_k^-
1	O6	0.0437	0.0961	-0.0699	0.0206	0.0454	0.4545	2.2004	-0.0330	0.1437	0.3162	-0.2299	-0.0022	0.1362
	N7	0.0845	-0.0519	-0.0163	0.0399	-0.0245	-1.6279	-0.6143	-0.0077	0.2779	-0.1707	-0.0536	0.1028	0.0007
	C12	0.0493	0.0008	-0.0251	0.0233	0.0004	60.3289	0.0166	-0.0119	0.1623	0.0027	-0.0825	0.1016	0.0006
	C19	-0.0090	0.1020	-0.0465	-0.0042	0.0482	-0.0878	-11.3879	-0.0220	-0.0295	0.3354	-0.1530	-0.0006	0.1408
	C25	0.0289	0.1397	-0.0843	0.0136	0.0660	0.2066	4.8408	-0.0398	0.0949	0.4595	-0.2772	-0.0052	0.2334
	C26	0.0909	0.0395	-0.0652	0.0430	0.0187	2.3016	0.4345	-0.0308	0.2990	0.1299	-0.2145	0.0278	0.0006
	C27	0.0530	0.0997	-0.0764	0.0251	0.0471	0.5322	1.8790	-0.0361	0.1745	0.3278	-0.2511	0.0143	0.0119
2	O4	0.1160	0.0471	-0.0815	0.0516	0.0210	2.4620	0.4062	-0.0363	0.2692	0.1093	-0.2681	0.1006	0.0354
	C13	0.0125	-0.0321	0.0230	0.0056	4.1239	0.2425	-0.0143	0.1198	0.0291	-0.1055	0.1120	0.0295	0.0125
	C14	0.0125	-0.0320	0.0229	0.0056	4.1167	0.2429	-0.0142	0.1193	0.0290	-0.1051	0.1219	0.0288	0.0125
	C16	0.0744	-0.0748	0.0334	0.0332	1.0088	0.9912	-0.0333	0.1743	0.1728	-0.2459	0.1059	0.0936	0.0744
	C17	0.1047	-0.0610	0.0077	0.0466	0.1655	6.0410	-0.0272	0.0402	0.2430	-0.2006	0.0002	0.0684	0.1047
	C22	0.0633	0.0339	-0.0486	0.0282	0.0151	1.8642	0.5364	-0.0216	0.1468	0.0788	-0.1598	0.1547	0.0609
	C23	0.0641	0.1050	-0.0845	0.0286	0.0467	0.6108	1.6373	-0.0376	0.1488	0.2436	-0.2780	0.0085	0.0842
	C24	0.0668	0.2486	-0.1577	0.0297	0.1107	0.2686	3.7234	-0.0702	0.1550	0.5770	-0.5186	0.0059	0.2392
3	C3	0.0520	0.1101	-0.0810	0.0285	0.0604	0.4720	2.1186	-0.0444	0.2723	0.5769	-0.4246	0.0006	0.1903
	C5	0.1333	0.0630	-0.0981	0.0731	0.0346	2.1149	0.4728	-0.0538	0.6983	0.3302	-0.5142	0.2887	0.0428
	C7	0.0664	0.0156	-0.0410	0.0364	0.0086	4.2426	0.2357	-0.0225	0.3478	0.0820	-0.2149	0.1601	0.0016
	C8	0.0011	0.1024	-0.0517	0.0006	0.0561	0.0104	95.7465	-0.0284	0.0056	0.5363	-0.2710	0.0037	0.1371
	O14	0.0588	0.1021	-0.0804	0.0322	0.0560	0.5757	1.7369	-0.0441	0.3080	0.5350	-0.4215	0.0470	0.1883
	C16	0.0913	0.0513	-0.0713	0.0501	0.0281	1.7810	0.5615	-0.0391	0.4785	0.2687	-0.3736	0.2010	0.0860
	C19	0.1146	0.0967	-0.1056	0.0628	0.0530	1.1845	0.8442	-0.0579	0.6004	0.5068	-0.5536	0.0893	0.1181
	C25	0.1094	0.0749	-0.0922	0.0600	0.0411	1.4594	0.6852	-0.0505	0.5731	0.3927	-0.4829	0.0487	0.0223
4	O2	0.0437	0.0761	-0.0599	0.0236	0.0411	0.5745	1.7406	-0.0324	0.1958	0.3408	-0.2683	0.0367	0.1223
	O4	0.1082	0.0103	-0.0592	0.0585	0.0056	10.5305	0.0950	-0.0320	0.4844	0.0460	-0.2652	0.1687	0.0111
	C12	-0.0099	0.0875	-0.0388	-0.0053	0.0472	-0.1131	-8.8426	-0.0210	-0.0443	0.3915	-0.1736	0.0061	0.1174
	C13	0.0963	0.0687	-0.0825	0.0520	0.0371	1.4017	0.7134	-0.0446	0.4311	0.3076	-0.3693	0.1727	0.0728
	C14	0.0179	0.1019	-0.0599	0.0097	0.0551	0.1760	5.6806	-0.0324	0.0803	0.4563	-0.2683	-0.0134	0.1912
	C18	0.0771	0.0468	-0.0619	0.0416	0.0253	1.6458	0.6076	-0.0335	0.3449	0.2096	-0.2773	0.2183	0.0869
	C22	0.1137	0.0534	-0.0835	0.0614	0.0289	2.1277	0.4700	-0.0451	0.5088	0.2391	-0.3740	0.0203	0.0116
5	O3	0.0842	0.0063	-0.0452	0.0404	0.0030	13.4216	0.0745	-0.0217	0.3062	0.0228	-0.1645	0.1285	0.0005
	C7	0.0601	-0.0120	-0.0240	0.0288	-0.0058	-4.9900	-0.2004	-0.0115	0.2186	-0.0438	-0.0874	0.1569	0.0100
	C10	0.0741	0.1561	-0.1151	0.0355	0.0749	0.4745	2.1075	-0.0552	0.2693	0.5674	-0.4184	0.1304	0.2673
	C11	0.0351	0.1037	-0.0694	0.0168	0.0498	0.3380	2.9590	-0.0333	0.1275	0.3772	-0.2524	0.0133	0.1570
	C12	0.0401	0.0936	-0.0668	0.0193	0.0449	0.4290	2.3313	-0.0321	0.1459	0.3402	-0.2430	0.0367	0.0699
	C19	0.0643	0.0279	-0.0461	0.0309	0.0134	2.3085	0.4332	-0.0221	0.2338	0.1013	-0.1675	0.1304	0.0039
	C20	0.1015	0.0405	-0.0710	0.0487	0.0194	2.5088	0.3986	-0.0341	0.3691	0.1471	-0.2581	0.0150	0.0006
6	O4	0.1260	0.0469	-0.0864	0.0598	0.0223	2.6856	0.3724	-0.0411	0.4572	0.1703	-0.3137	0.1055	0.0009
	C9	0.0562	-0.0037	-0.0263	0.0267	-0.0017	-15.3630	-0.0651	-0.0125	0.2039	-0.0133	-0.0953	0.1442	0.0190
	C11	0.0864	0.1593	-0.1228	0.0410	0.0757	0.5422	1.8444	-0.0584	0.3136	0.5784	-0.4460	0.1342	0.3694
	C19	0.0729	0.0326	-0.0528	0.0346	0.0155	2.2335	0.4477	-0.0251	0.2647	0.1185	-0.1916	0.1361	0.0057
7	O3	0.0640	0.0102	-0.0371	0.0308	0.0049	6.2678	0.1595	-0.0179	0.2485	0.0396	-0.1441	0.0908	0.0004
	O8	0.0949	0.0470	-0.0709	0.0457	0.0227	2.0163	0.4960	-0.0342	0.3683	0.1827	-0.2755	0.0666	0.0006
	C14	0.0432	0.1737	-0.1085	0.0208	0.0837	0.2490	4.0165	-0.0522	0.1679	0.6745	-0.4212	0.0249	0.4411
	C20	0.0541	0.0304	-0.0422	0.0260	0.0146	1.7776	0.5626	-0.0203	0.2099	0.1181	-0.1640	0.1179	0.0058
	C21	0.0862	0.0550	-0.0706	0.0415	0.0265	1.5655	0.6388	-0.0340	0.3346	0.2138	-0.2742	0.0117	0.0011

3.6 Molecular docking

Molecular docking is a fairly efficient technique for predicting the binding sites in the ligand receptor interaction [43]. The blind docking has been performed to examine the bio-activity of compounds (1-7) against 6LU7 by first cleaning the target. The size of the grid with spacing 1 Å was so as to cover up the target protein. The numerical value of binding energy(B.E.) and ligand efficiency(η) should be higher for better binding of ligand with receptor [43]. Also the ligand possessing

more number of H bonds with small bond length are more suitable molecule. The inhibition constant (K_I) indirectly measures the changes in enzyme kinetics and should have low value for improved docking. The root mean square deviation (RMSD) deals with the mean distance between atoms of protein and ligand [44,45]. All the docking parametersand pose for the seven molecules with the bonded residues of 6LU7 are summarizedin Table 4 and Figure 4, respectively. The bioactivity of a molecule is governed by the strength and number of hydrogen bonds formed with the receptor protein. The maximum number of H bonds, having smallest bond length of 2.13 Å between residue A: GLU166 of 6LU7 and O1 atom were formed in compound 6.(Table 4 and Figure 4). The highest value K_I was estimated at 0.33 for compound 3, 5 and 6. Also, the minimumη and maximum B.E. of 12.56 μM, and 6.69 kcal/ mole, respectively were calculatedfor compound 6. Hence compound 6 is the most suitable inhibitor among the seven selected molecules.

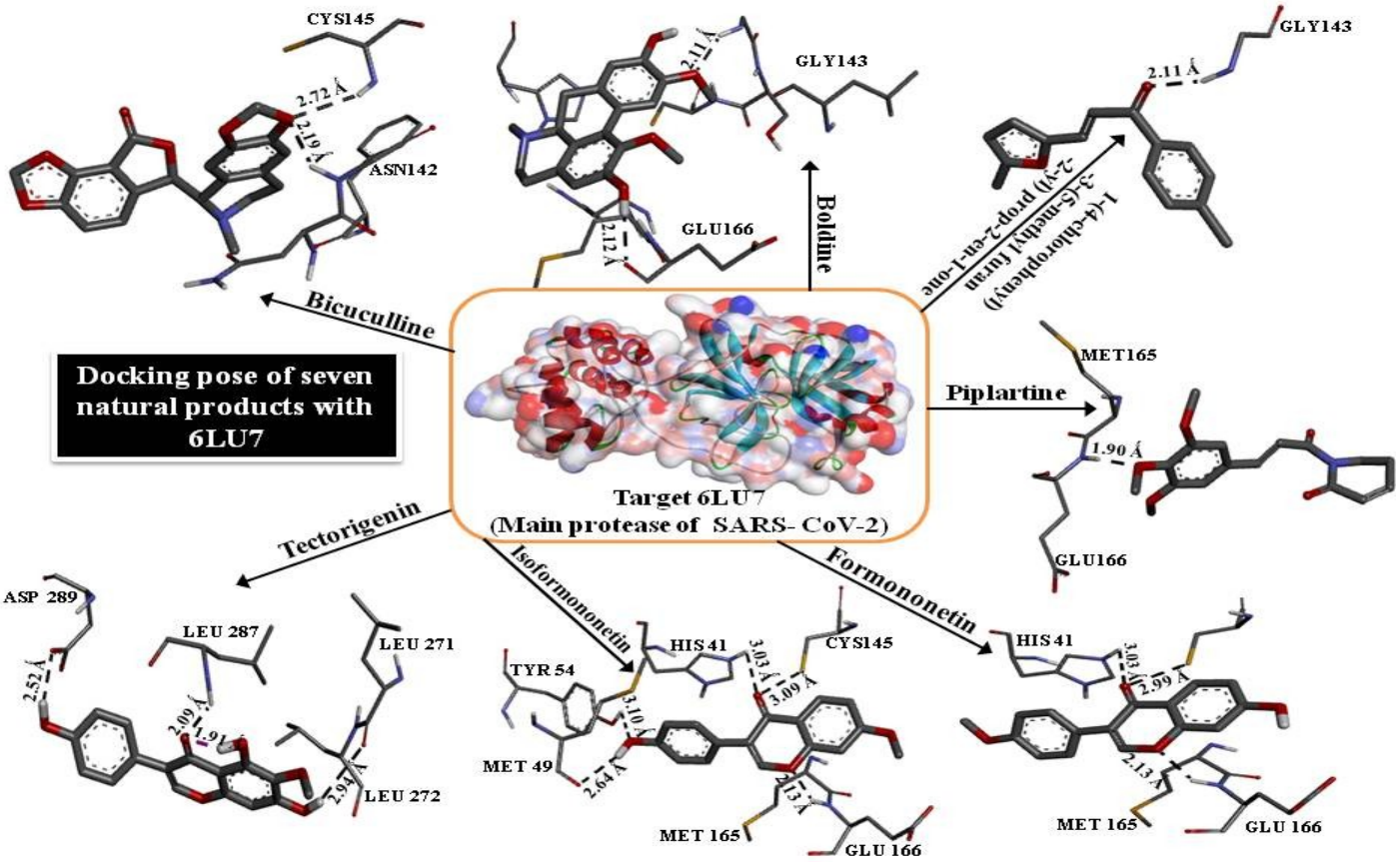

Figure 4 Docking poses of compounds (1-7) with 6LU7.

Table 4
Molecular docking parameters compounds (1-7) with 6LU7.

Comp.	Bonded Residue	Bond length (Å)	Inhibition Constant (μM)	Binding energy (kcal/mol)	Reference RMSD (Å)	Ligand efficiency
1.	A:GLY143 A:CYS145	2.19 2.72	65.34	5.71	70.645	0.21
2.	A:GLY143 A:GLU166	2.11 2.12	41.14	5.98	71.279	0.25
3.	A:GLY143	2.11	81.80	5.58	70.357	0.33
4.	A:GLU166	1.90	492.38	4.51	74.970	0.21
5.	A:HIS41 A:CYS145	3.03 2.99	15.20	6.57	71.317	0.33

	A:GLU166	2.18				
6.	A:HIS41	3.03	12.56	6.69	71.456	0.33
	A:TYR54	3.10				
	A:CYS145	3.09				
	A:GLU166	2.13				
	A:MET49	2.64				
7.	A:LEU287	2.09	499.86	4.50	67.550	0.20
	A:ASP289	2.52				
	A:LEU271	2.94				

4. Conclusion

The DFT study, incorporating graphical and topological analysis, accompanied by molecular docking is extremely convincing technique for the study of structural prop- erties and binding ability of organic compounds. The calculated values of $Log_{10}P$, MR, number of H bond donor and acceptor have confirmed the drug character of all the selected compounds. The global reactivity parameters have declared that compound 3 and 2 are most reactive and stable structure, respectively. The expected nucleophilic and electrophilic sites for the seven molecules were examined through MESP plot and local reactivity descriptors evaluation. Molecular docking studies verified the similar activity sites. It has been further concluded that molecule 6 (Isoformononetin) having best docking for 6LU7 among the seven selected natural products, could be a potentialprospect for the treatment of COVID-19, however the in-vitro and in-vivo analyseswill have to validate the same.

Acknowledgement

Poonam Tandon thanks DST-SERB for financial support under project (grant no. CRG/2019/006670).

References

[1] Wu, Y., Ho, W., Huang, Y., Jin, D. Y., Li, S., Liu, S. L., ... & Yuen, K. Y. (2020). SARS-CoV-2 is an appropriate name for the new coronavirus. The Lancet, 395(10228), 949-950.
[2] https://www.euro.who.int/en/health-topics/health-emergencies/coronavirus-covid-19/novel-coronavirus-2019-ncov: accessed 01/07/2021
[3] Huang, J., Tao, G., Liu, J., Cai, J., Huang, Z., & Chen, J. X. (2020). Current prevention of COVID-19: natural product and herbal medicine. Frontiers in Pharmacology, 11, 1635.
[4] Wang, Z., & Yang, L. (2020). Turning the Tide: Natural Products and Natural-Product-Inspired Chemicals as Potential Counters to SARS-CoV-2 Infection. Frontiers in Pharmacology, 11.
[5] Da Silva Antonio, A., Wiedemann, L. S. M., & Veiga-Junior, V. F. (2020). Natural products' role against COVID-19. RSC Advances, 10(39), 23379-23393.
[6] Narkhede, R. R., Pise, A. V., Cheke, R. S., & Shinde, S. D. (2020). Recognition of natural products as potential inhibitors of COVID-19 main protease (Mpro): In-silico evidences. Natural Products and Bioprospecting, 10(5), 297-306.
[7] Boozari, M., & Hosseinzadeh, H. (2020). Natural products for COVID-19 prevention and treatment regarding to previous coronavirus infections and novel studies. Phytotherapy Research.
[8] Srivastava, A., Rawat, P., Tandon, P., & Singh, R. N. (2012). A computational study on conformational geometries, chemical reactivity and inhibitor property of an alkaloid bicuculline with γ-aminobutyric acid (GABA) by DFT. Computational and Theoretical Chemistry, 993, 80-89.
[9] Srivastava, A., Tandon, P., Ayala, A. P., & Jain, S. (2011). Solid state characterization of an antioxidant alkaloid boldine using vibrational spectroscopy and quantum chemical calculations. Vibrational Spectroscopy, 56(1), 82-88.
[10] Shukla, S., Srivastava, A., Srivastava, K., Tandon, P., Jamalis, J., & Singh, R. B. (2020). Non-covalent interactions and spectroscopic study of chalcone derivative 1-(4-chlorophenyl)-3-(5-methylfuran-2-yl) prop-2-en-1-one. Journal of Molecular Structure, 1201, 127145.

[11] Srivastava, A., Karthick, T., Joshi, B. D., Mishra, R., Tandon, P., Ayala, A. P., & Ellena, J. (2017). Spectroscopic (far or terahertz, mid-infrared and Raman) investigation, thermal analysis and biological activity of piplartine. Spectrochimica Acta Part A: Molecular and Biomolecular Spectroscopy, 184, 368-381.
[12] Srivastava, A., Mishra, R., Kumar, S., Dev, K., Tandon, P., & Maurya, R. (2015). Molecular structure, spectral investigation (1H NMR, 13C NMR, UV–Visible, FT-IR, FT-Raman), NBO, intramolecular hydrogen bonding, chemical reactivity and first hyperpolarizability analysis of formononetin [7-hydroxy-3 (4-methoxyphenyl) chromone]: A quantum chemical study. Journal of Molecular Structure, 1084, 55-73.
[13] Srivastava, A., Singh, H., Mishra, R., Dev, K., Tandon, P., & Maurya, R. (2017). Structural insights, protein-ligand interactions and spectroscopic characterization of isoformononetin. Journal of Molecular Structure, 1133, 479-491.
[14] Shukla, S., Srivastava, A., Kumar, P., Tandon, P., Maurya, R., & Singh, R. B. (2020). Vibrational spectroscopic, NBO, AIM, and multiwfn study of tectorigenin: A DFT approach. Journal of Molecular Structure, 128443.
[15] Lipinski, C. A. (2000). Drug-like properties and the causes of poor solubility and poor permeability. Journal of pharmacological and toxicological methods, 44(1), 235-249.
[16] Sanders, J. M., Monogue, M. L., Jodlowski, T. Z., & Cutrell, J. B. (2020). Pharmacologic treatments for coronavirus disease 2019 (COVID-19): a review. Jama, 323(18), 1824-1836.
[17] Kohn, W., & Sham, L. J. (1965). Self-consistent equations including exchange and correlation effects. Physical review, 140(4A), A1133.
[18] Frisch, M. J., Trucks, G. W., Schlegel, H. B., Scuseria, G. E., Robb, M. A., Cheeseman, J. R., ... & Nakatsuji, H. (2009). Gaussian 09; Gaussian, Inc. Wallingford, CT, 32, 5648-5652.
[19] Becke, A. D. (1993). Becke's three-parameter hybrid method using the LYP correlation functional. J. Chem. Phys, 98(492), 5648-5652.
[20] Lee, C., Yang, W., & Parr, R. G. (1988). Development of the Colle-Salvetti correlation-energy formula into a functional of the electron density. Physical Review B, 37(2), 785.
[21] Miehlich, B., Savin, A., Stoll, H., & Preuss, H. (1989). Results obtained with the correlation energy density functionals of Becke and Lee, Yang, and Parr. Chemical Physics Letters, 157(3), 200-206.
[22] E. Frisch, H. P. Hratchian, R. D. Dennington II, T. A. Keith, J. Millam, B. Nielsen, A. J. Holder, and J. Hiscocks, GaussView Version 5. 0. 8, Gaussian, Inc., 2009.
[23] Forli, W., Halliday, S., Belew, R., & Olson, A. J. (2012). AutoDock Version 4.2.
[24] Wang, J., Kollman, P. A., & Kuntz, I. D. (1999). Flexible ligand docking: a multistep strategy approach. Proteins: Structure, Function, and Bioinformatics, 36(1), 1-19.
[25] Gasteiger, J., & Marsili, M. (1980). Iterative partial equalization of orbital electronegativity—a rapid access to atomic charges. Tetrahedron, 36(22), 3219-3228.
[26] Dassault Systèmes BIOVIA (2015) Discovery studio modeling environment, release 4.5. Dassault Systèmes BIOVIA, San Diego.
[27] Rice, J. E. (2014). Organic Chemistry Concepts and Applications for Medicinal Chemistry. Academic Press.
[28] Leo, A., & Hoekman, D. H. (1995). *Exploring QSAR.: Fundamentals and applications in chemistry and biology* (Vol. 1). American Chemical Society.
[29] Atkin, P. W., & de Paula, J. (2002). Physical Chemistry, edited by WH Freeman. *New York, NY*.
[30] Atkins, P., & De Paula, J. (2011). Physical chemistry for the life sciences. Oxford University Press, USA.
[31] Jacquemin, D., & Perpète, E. A. (2007). On the basis set convergence of TD-DFT oscillator strengths: Dinitrophenylhydrazones as a case study. Journal of Molecular Structure: THEOCHEM, 804(1-3), 31-34.
[32] Parr, R. G., Szentpaly, L. V., & Liu, S. (1999). Electrophilicity index. Journal of the American Chemical Society, 121(9), 1922-1924.
[33] P. K. Chattaraj, S. Giri, The Journal of Physical Chemistry A 111, no. 43 (2007): 11116-11121.
[34] Pearson, R. G. (1990). Hard and soft acids and bases—the evolution of a chemical concept. Coordination chemistry reviews, 100, 403-425.
[35] Parr, R. G., & Yang, W. (1984). Density functional approach to the frontier-electron theory of chemical reactivity. Journal of the American Chemical Society, 106(14), 4049-4050.
[36] Murray, J. S., & Sen, K. (Eds.). (1996). Molecular electrostatic potentials: concepts and applications. Elsevier.

[37] Domingo, Luis R., Mar Ríos-Gutiérrez, and Patricia Pérez. "Applications of the conceptual density functional theory indices to organic chemistry reactivity." *Molecules* 21, no. 6 (2016): 748.
[38] Yang, W., & Mortier, W. J. (1986). The use of global and local molecular parameters for the analysis of the gas-phase basicity of amines. Journal of the American Chemical Society, 108(19), 5708-5711.
[39] Roy, R. K., Krishnamurti, S., Geerlings, P., & Pal, S. (1998). Local softness and hardness based reactivity descriptors for predicting intra-and intermolecular reactivity sequences: carbonyl compounds. The Journal of Physical Chemistry A, 102(21), 3746-3755.
[40] Domingo, L. R., Aurell, M. J., Pérez, P., & Contreras, R. (2002). Quantitative characterization of the local electrophilicity of organic molecules. Understanding the regioselectivity on Diels− Alder reactions. The Journal of Physical Chemistry A, 106(29), 6871-6875.
[41] Domingo, L. R., Pérez, P., & Sáez, J. A. (2013). Understanding the local reactivity in polar organic reactions through electrophilic and nucleophilic Parr functions. RSC advances, 3(5), 1486-1494.
[42] Chamorro, E., Pérez, P., & Domingo, L. R. (2013). On the nature of Parr functions to predict the most reactive sites along organic polar reactions. Chemical Physics Letters, 582, 141-143.
[43] Matta, C. F., Hernández-Trujillo, J., Tang, T. H., & Bader, R. F. (2003). Hydrogen–hydrogen bonding: a stabilizing interaction in molecules and crystals. Chemistry–A European Journal, 9(9), 1940-1951.
[44] Gohlke, H., & Klebe, G. (2002). Approaches to the description and prediction of the binding affinity of small-molecule ligands to macromolecular receptors. Angewandte Chemie International Edition, 41(15), 2644-2676.
[45] Meng, X. Y., Zhang, H. X., Mezei, M., & Cui, M. (2011). Molecular docking: a powerful approach for structure-based drug discovery. Curr Comput Aided Drug Des 7: 146–157.